

Model-based prediction of fluid bed state in full-scale drinking water pellet softening reactors

O.J.I. Kramer^{*/**}, M.A. Jobse^{*/**}, E.T. Baars^{*}, A.W.C. van der Helm^{*/***}, M.G. Colin^{*}, L.J. Kors^{*} & W.H. van Vugt^{**}

* Waternet, PO Box 94370, 1090 GJ, Amsterdam, the Netherlands, (E-mail: onno.kramer@waternet.nl), Tel: +31 6-52480035

** HU University of Applied Sciences Utrecht, Institute for Life Science and Chemistry, PO Box 12011, 3501 AA Utrecht, The Netherlands

*** Delft University of Technology, Faculty of Civil Engineering and Geosciences, Department of Water Management, PO Box 5048, 2600 GA, Delft, the Netherlands

ABSTRACT

Softening at drinking water treatment plants is often realised by fluidised bed pellet reactors. Generally, sand is used as seeding material and pellets are produced as a by-product. To improve to sustainability, research has been carried out to replace the seeding material by re-using grained and sieved calcite pellets as seeding material. An explicit fluidisation model is developed to predict the fluid bed state in fluid bed pellet softening reactors with calcite as seeding material.

The fluidisation theory is extended in a model whereby soft sensors are derived and experimentally tested for a wide range of seeding material and pellets. With the soft sensors porosity, particle size and pressure drop can explicitly be calculated. Pilot research has been carried out to calibrate and full-scale experiments to validate the fluidisation models.

Four different fluidisation models were reviewed from which the original Richardson-Zaki fluid bed model has been selected as the best explicit fluidisation model to predict the porosity, particle size and pressure drop. Applying a discretisation model for the fluid bed pellet reactor, the current operation of the treatment softening can be improved by estimating the fluidisation, pressure drop behaviour and particle profile.

Waternet can apply the Richardson-Zaki fluid bed model in practice for building a soft sensor to achieve optimal bed fluid conditions for the softening process.

Keywords: calcite, carmán-közény, drinking water, ergun, fluidisation, garnet pellets, modelling, pellet softening, process optimisation, richardson-zaki, soft sensor, terminal settling

INTRODUCTION

Softening process

Pellet softening in a fluid bed reactor was developed and introduced in the late 80's in the Netherlands^[20]. In 2016 almost all drinking water in the Netherlands will be softened by fluidised bed pellet reactor^[37]. Caustic soda, soda ash or lime is dosed in a cylindrical reactor in up flow, resulting in exceeding the calcium carbonate equilibrium. The reactor is filled with seeding material and pellets so crystallisation will be the predominant process. Garnet sand and crystal sand grains are known as suitable seeding material. The large specific surface area in the reactor causes the CaCO₃ to crystallise^[14] on the particles called pellets and therefore grow in size.

Sustainability

Frequently the largest pellets (depending on the required set-point but in general larger than 1-2 mm) are withdrawn from the reactor and are used as a by-product^[13] in other processes e.g. industrial and agricultural processes^[18]. The garnet core inside the pellets, inhibits high potential market segments such as glass, paper, food and feed and inhibits direct re-use in the pellet reactor itself for a more sustainable and circular process. Increasing the pellet market value and sustainability of the softening process can be achieved through the substitution of the sand grain with a calcite grain of 0.5 mm (100% calcium carbonate). If the calcite pellets are grinded and sieved they can be re-used as a seeding material. This circular economy principle contributes to the sustainability objectives of Waternet, the water cycle utility of Amsterdam and surrounding areas in the Netherlands.

Prediction of the fluid bed state

The softening process of Waternet requires frequent adjustments of the process settings for controlling fluidisation and pellet size, due to seasonal changes of water temperature since surface water is used for production of drinking water. Due to advanced automation, the overall process control requires a high standard within limited margins. For garnet as seeding material, fluidisation behaviour models^{[22][30]} for pellets have been described. For pellets based on calcite as seeding material no suitable model currently exists. An important parameter in the softening process is the bed porosity from which further performance indicators can be derived. This bed porosity is mostly obtained indirectly. Based on known process parameters i.e. water flow, water temperature, bed height, pressure drop and reactor characteristics and the fluidisation theory the porosity can be calculated.

The average particle size of the pellets at the bottom of the reactor is used for adjustments to the process. The particle profile in the operating reactor must be obtained through taking samples and sieve analysis. This is a time-consuming activity and not fully adequate for optimising the reactor softening conditions. Therefore, real-time soft sensors are desired.

The objective of this study is to develop an explicit fluidisation model to predict the fluid bed state in fluid bed pellet softening reactors with calcite as seeding material.

MATERIAL AND METHODS

The existing theory is used to predict the porosity, the pressure drop over 50 cm and average particle size. A calibrated and validated fluid bed model is developed for prediction optimal fluid bed conditions.

Review of fluidisation and terminal settling theory

In predicting the fluidisation behaviour of garnet pellets, earlier research^[30] provided several models which could be used to control the fluid bed pellet softening reactors. Comprehensive fluidisation theory^{[26][40][5][8]} is available in the literature. Most articles use filtration based fluidisation fundamentals by Ergun^[15] based on forces acting on particles, or the settling based fluidisation by Richardson-Zaki^{[27][28]}. Many models^[43] have been developed and are modifications of Ergun, Richardson-Zaki or the Carmán-Közény correlation. With the filtration based fixed bed models the pressure drop can be estimated in which the settling based models are suitable for predicting the fluidised bed porosity. In the steady state of homogeneous fluidisation, the pressure drop^{[43][16][41]} equals the buoyance according to Equation 1:

$$\frac{\Delta P}{\Delta L} = (1 - \varepsilon)(\rho_p - \rho_f)g \quad (1)$$

Through using Equation 1 the filtration based models can be rewritten and used for the fluid bed state. Above theory is based on filtration principles. Another approach has been made by Richardson and Zaki^{[43][42]} with Equation 2:

$$\frac{v_l}{v_{t,(\varepsilon \rightarrow 1)}} = \varepsilon^{n_{RZ}} \quad (2)$$

It has been found that $v_{t,(\varepsilon \rightarrow 1)}$ corresponds closely to the free falling velocity v_t of a particle in an infinite medium.

According to literature^{[8][12]} the index $n = n_{RZ}$ in Equation 2 also can be obtained by neglecting the wall effects according to Equation 3:

$$n_{RZ} = \frac{\log\left(\frac{v_l}{v_t}\right)}{\log(\varepsilon)} \quad (3)$$

Here settling theory^{[22][7][6]} is the fundamental base of the Richardson-Zaki model to analytically obtain the porosity. The coefficient n_{RZ} , often called the hindering factor, is known for both complete laminar and turbulent regime. In literature^{[8][12]} the laminar flow states $n_{RZ}=4.8$ and for turbulent flow $n_{RZ}=2.4$. This is in analogue with the filtration theory of Ergun and the settling theory of Richardson-Zaki. Since complete

laminar and turbulent conditions are not the case in practice, many equations^{[35][8]} are given to calculate the index n_{RZ} as a function of Reynolds terminal number Re_t :

$$n_{RZ} = \begin{cases} Re_t < 0.2 & n_{RZ} = 4.65 + 19.5 \frac{d_p}{D} \\ 0.2 < Re_t < 1 & n_{RZ} = 4.35 + 17.5 \frac{d_p}{D} Re_t^{-0.03} \\ 1 < Re_t < 200 & n_{RZ} = 4.45 + 18 \frac{d_p}{D} Re_t^{-0.1} \\ 200 < Re_t < 500 & n_{RZ} = 4.45 Re_t^{-0.1} \\ Re_t > 500 & n_{RZ} = 2.39 \end{cases} \quad (4)$$

The Reynolds number, under terminal falling conditions, states:

$$Re_t = \frac{d_p \rho_f v_{t(\varepsilon \rightarrow 1)}}{\mu} \quad (5)$$

Many other relations exist^{[1][35][9]} for the Reynold number but also the following equation proposed by Rowe^{[29][43][16][12]} can be used:

$$\frac{4.8 - n_{RZ}}{n_{RZ} - 2.4} = \alpha Re_t^\beta \quad (6)$$

n_{RZ} can be calculated using α en β and the Reynolds number in Equation 6. In the literature^{[11][43][35]} $\alpha=0.175$ and $\beta=0.75$ can be found as one of the countless correlation parameters.

The disadvantage of Equation 6 is that the terminal velocity is also used in the Richardson-Zaki Equation 2 which, results in an implicit model. Implicit models are not eligible in full scale process automation due to the risk of jamming numerical loops. Therefore, another method is the introduction of the dimensionless particle diameter or the Archimedes number 7 sometimes also called the Galileo number:

$$Ar = \frac{gd_p^3 \rho_f (\rho_p - \rho_f)}{\mu^2} \quad (7)$$

Analogue to Equation 6, Equation 8 of Khan and Richardson^{[21][16][8]} for n_{RZ} is given:

$$\frac{4.8 - n_{RZ}}{n_{RZ} - 2.4} = \alpha Ar^\beta \quad (8)$$

Now the index n_{RZ} can be calculated and the porosity explicitly given^[43] for $\alpha=0.043$ and $\beta=0.57$.

According to^[35] n_{RZ} can exceed the value of 4.8 in some cases e.g. in case of sand or natural grains. A more suitable equation can be derived from expression 4 like Equation 9:

$$n_{RZ} = a_1 Re_t^{a_2} \quad (9)$$

Several coefficients^[35] have been given e.g. sand $a_1=7.08$ and $a_2=-0.196$ and for diatomite $a_1= 8.41$ and $a_2=-0.179$.

The analytical equation for the drag force on the particle states:

$$C_D = \frac{4}{3} \frac{gd_p}{v_{t(\varepsilon \rightarrow 1)}^2} \frac{(\rho_p - \rho_f)}{\rho_f} \quad (10)$$

Countless semi-analytical equation for C_D exist in which often is the Rowe equation is used^{[26][31][43][34][36]}:

$$C_D = \frac{24}{Re_t} \left(1 + \alpha Re_t^\beta \right) \quad (Re_t < 1000) \quad (11)$$

The terminal particle settling velocity can be derived from Equation 10 and then equals Equation 11. From literature^[22] $\alpha=0.15$ and $\beta=0.687$.

According to Turton & Levenspiel^[36] the drag can be predicted accurately with Equation 12:

$$C_D = \frac{24}{Re_t} \left(1 + 0.173 Re_t^{0.657} + \frac{0.413}{1 + 16300 Re_t^{-1.09}} \right) \quad (Re_t < 1000) \quad (12)$$

However an implicit equation for the porosity results. A explicit solution for the porosity can be found with Equation 13 where the coefficients α and β can be determined by plotting the logarithmical drag against the logarithmical terminal Reynolds number^[43]. The equation becomes:

$$C_D = \alpha Re_t^\beta \quad (13)$$

$$\ln C_D = \ln \alpha + \beta \ln(Re_t) \quad (14)$$

However, Equations 11, 13 and 14 do not cover the whole range of Reynolds terminal well enough. The correlation between $\log C_D$ and $\log Re_t$ isn't completely linear.

Therefore an improved approach is proposed in this study using the Archimedes number:

$$\ln \hat{u} = \ln \alpha + \beta \ln(Ar) \quad (15)$$

In which \hat{u} presents the dimensionless particle terminal settling velocity^[10] according to Equation 16:

$$\hat{u} = \frac{\rho_f^2 v_{t(\varepsilon \rightarrow 1)}^3}{(\rho_p - \rho_f) g \mu} \quad (16)$$

Another relation between Reynolds terminal and Archimedes is^[43]:

$$\ln Re_t = c_1 + c_2 \ln(Ar) \quad (17)$$

or:

$$Re_t = e^{c_1} Ar^{c_2} \quad (18)$$

Combining Equation 9 and 18 gives Equation 19:

$$n_{RZ} = a_1 e^{c_1 a_2} Ar^{c_2 a_2} \quad (19)$$

Now the porosity can be calculated explicitly using Equation 2 and 19 and.

Predicting models

Four different models have been derived to respectively determine fluid bed porosity, pressure drop and average particle size at the bottom of the pellet reactor. The goal is to acquire an explicit form of the correlation but this is not always possible.

With the total pressure difference over the reactor bed, the total bed mass can be calculated and the amount of calcium carbonate which crystallises at the particles in time can be monitored. With the estimated bed porosity, together with the predicted average particle size, the specific surface area and space velocity can be calculated and information about the fluid bed performance can be acquired.

Ergun model

Predicting pressure drop

Ergun^[15] present the following equation^[16] for the pressure drop according to Equation 20.

$$\frac{\Delta P}{\Delta L} = 150 \frac{\mu v_l}{(d_p \phi_s)^2} \frac{(1-\varepsilon)^2}{\varepsilon^3} + \frac{7}{4} \frac{\rho_f v_l^2}{d_p \phi_s} \frac{(1-\varepsilon)}{\varepsilon^3} \quad (20)$$

The sphericity ϕ_s has been examined in this research to according the Wen-Yu^{[41][43]} Equations 21 and 22, but did not improve the prediction and are therefore are not taken into account. See Table 9.

$$\phi_s = \frac{1}{\varepsilon_{mf}^3} \quad (21)$$

$$\phi_s = \sqrt{\frac{1-\varepsilon_{mf}}{11 \varepsilon_{mf}^3}} \quad (22)$$

An alternative equation has been given by Limas-Ballesteros^[4]:

$$\phi_s^{0.376} = \frac{0.42}{\varepsilon_{mf}^3} \quad (23)$$

Predicting fluid bed porosity

Equation 20 combined with Equations 1 into 24 cannot be rewritten into an explicit relation for the bed porosity and must be solved using an iteration solver.

$$\frac{\Delta P}{\Delta L} = (1 - \varepsilon)(\rho_p - \rho_f)g = 150 \frac{\mu v_l (1-\varepsilon)^2}{(d_p \phi_s)^2 \varepsilon^3} + \frac{7}{4} \frac{\rho_f v_l^2 (1-\varepsilon)}{d_p \phi_s \varepsilon^3} \quad (24)$$

Predicting average particle size

Assuming that the particles in the lowest reactor section of 50 cm are uniform, the measurement of the pressure drop e.g. ΔP_{50} over 50 cm of the reactor is an indirect indication of the pellet size^[31] of the reactor. Therefore the pressure drop, combined with the water flow and temperature, is a soft sensor for the pellet size which can be used to control the optimal pellet diameter by automatically removal of pellets from the reactor in case a set-point for the ΔP_{50} is exceeded.

Both the Ergun Equation 20 and the Ergun adjusted equation can be rewritten for explicit Equation 25 for the particle diameter d_p as a function of $\Delta P/L$:

$$d_p = \frac{1}{2 \frac{\Delta P}{\Delta L}} \left(q + \sqrt{q^2 + 4p \frac{\Delta P}{\Delta L}} \right) \quad (25)$$

p and q for Ergun states:

$$p = 150 \mu v_l \frac{(1-\varepsilon)^2}{\varepsilon^3} \quad (26)$$

$$q = \frac{7}{4} \rho_f v_l^2 \frac{(1-\varepsilon)}{\varepsilon^3} \quad (27)$$

Assuming the particle size distribution is uniform, the bed porosity can be acquired in case the pressure drop over 50 cm is known:

$$\varepsilon = 1 - \frac{\frac{\Delta P}{\Delta L}}{(\rho_p - \rho_f)g} \quad (28)$$

Ergun adjusted model

Predicting pressure drop

The Ergun model is often adjusted^{[16][17]} and some assumptions have been made for tortuosity, friction factor and pressure drop with corrections derived from practical experiences. Another form of Ergun equation^[43] is the Ergun-adjusted relation according for the pressure drop:

$$\frac{\Delta P}{\Delta L} = 18 \frac{\mu v_l (1-\varepsilon)}{(d_p \phi_s)^2 \varepsilon^{4.8}} + 0.33 \frac{\rho_f v_l^2 (1-\varepsilon)}{d_p \phi_s \varepsilon^{4.8}} \quad (29)$$

Predicting fluid bed porosity

If Equation 1 and 29 are combined an explicit relation is derived for the bed porosity. The simplified Ergun-adjusted Equation 30 becomes:

$$\varepsilon^{4.8} = 18 \frac{\mu v_l}{(d_p \phi_s)^2 (\rho_p - \rho_f) g} + 0.33 \frac{\rho_f v_l^2}{(d_p \phi_s) (\rho_p - \rho_f) g} \quad (30)$$

The coefficient n_{EA} is introduced and has a value of $n_{EA}=4.8$ in Equation 30 but can be calibrated for experimental data.

Predicting average particle size

To estimate the average particle diameter the Ergun Equation 25 can also be used whereby p and q for Ergun-Adjusted, states:

$$p = 18 \mu v_l \frac{(1-\varepsilon)}{\varepsilon^{4.8}} \quad (31) \quad q = 0.33 \rho_f v_l^2 \frac{(1-\varepsilon)}{\varepsilon^{4.8}} \quad (32)$$

Carmán-Közény model

Predicting pressure drop

The Carmán-Közény equation for the pressure drop used in literature^{[43][8]} is:

$$\frac{\Delta P}{\Delta L} = 180 \frac{v_l \mu (1-\varepsilon)^2}{d_p^2 \varepsilon^3} \quad (33)$$

Introducing the Reynolds number in Equation 34 which is corrected for the porosity, states:

$$Re_\varepsilon = \frac{\rho_f d_p v_l}{\mu} \frac{1}{(1-\varepsilon)} \quad (34)$$

Equation 33 becomes after defining a drag coefficient^[30] f:

$$f \approx \frac{36 K_{CK}}{Re_\varepsilon^n} \quad (35)$$

$$\frac{\Delta P}{\Delta L} = 36 \frac{K_{CK}}{Re_\varepsilon^n} \frac{\rho_f v_l^2 (1-\varepsilon)}{d_p \varepsilon^3} \quad (36)$$

The index $n = n_{CK}$ is introduced, in which for laminar flow $n_{CK}=1$ and $K_{CK}=5$. For laminar-turbulent region^{[8][13][26]} $n_{CK}=0.8$ and $K_{CK}=3.61$. This relation can also be rewritten into Equation 37:

$$\frac{\Delta P}{\Delta L} = 36 K_{CK} \frac{\mu^n \rho_f^{1-n} v_l^{2-n} (1-\varepsilon)^{n+1}}{d_p^{n+1} \varepsilon^3} \quad (37)$$

Predicting fluid bed porosity

If equation 1 and 37 are combined into the Montgomery^[24] equation 38 as well the relation is derived for the bed porosity and can be solved numerically.

$$\frac{\varepsilon^3}{(1-\varepsilon)^n} = 36K_{CK} \frac{\mu^n \rho_f^{1-n}}{g(\rho_p - \rho_f)} \frac{v_l^{2-n}}{d_p^{n+1}} \quad (38)$$

Predicting average particle size

The Carmán-Közény Equation 37 can be used to predict the average particle diameter according Equation 39:

$$d_p^{n+1} = 36K_{CK} \frac{\mu^n \rho_f^{1-n}}{g(\rho_p - \rho_f)} \frac{(1-\varepsilon)^n}{\varepsilon^3} v_l^{2-n} \quad (39)$$

Richardson-Zaki model

Predicting pressure drop

The Richardson-Zaki equation for the estimation of the pressure drop can be substituting 1, 2, 5, and 7 in Equation 18 resulting in 40 for the pressure difference in the fluid bed state:

$$\frac{\Delta P}{\Delta L} = \frac{(\rho_p - \rho_f)^{c_2+1} g^{c_2+1} (1-\varepsilon)^n d_p^{3c_2-1} e^{c_1}}{\mu^{2c_2-1} v_l \rho_f^{1-c_2}} \quad (40)$$

n_{RZ} can be derived with Equation 9.

Predicting fluid bed porosity

Based on the physical properties of the particles, the seeding material and the fluid, the dimensionless diameter Archimedes using Equation 7 is calculated. Based on the linear correlation 17 or 15 the dimensionless velocity or Reynolds terminal can be found. According to Equations 16 and 5. With Equation 9, the hindering coefficient is known and using Equation 2 the porosity can be calculated using Equation 41 for the fluid bed porosity:

$$\varepsilon^n = \frac{\mu^{(2c_2-1)} \rho_f^{(1-c_2)} v_l}{e^{c_1} g^{c_2} (\rho_p - \rho_f)^{c_2} d_p^{3c_2-1}} \quad (41)$$

Herewith a clear relation is established between the fluid bed porosity ε and the particle diameter d_p .

Predicting average particle size

Rewriting Equation 41 gives Equation 42 for the average particle diameter:

$$d_p^{3c_2-1} = \frac{\mu^{(2c_2-1)} \rho_f^{(1-c_2)} v_l}{\varepsilon^n e^{c_1} (\rho_p - \rho_f)^{c_2} g^{c_2}} \quad (42)$$

The Richardson-Zaki Equation 42 and the Carmán-Közény Equation 37 are different expressions however they have the same units for all parameters for the following coefficients: $n_{CK}=1$, $K_{CK}=5$ and $c_1=1$, $c_2=1$ and $n_{RZ}=2$.

The comparison of theoretical models requires information on fluidisation and terminal settling behaviour of solid grains.

Experimental setup

Several pilot and full scale experiments^[32] were carried out in the Weesperkarspel drinking water treatment and pilot plant of Waternet, located in Amsterdam, the Netherlands. The raw water originates from seepage water from the Bethune polder. The water is pre-treated by coagulation and sedimentation, followed by approximately 90 days retention in a lake reservoir. Subsequently it is filtered through rapid sand filters. The treatment plant that follows contains ozonation, pellet softening, biological activated carbon filtration and slow sand filtration. Chlorination is not needed.

A full scale test^[23] is started in the beginning of 2014 with the transition from garnet sand as a seeding material to Italian calcite, pure CaCO_3 , as a seeding material. The full scale test also includes the grinding and sieving of the extracted calcite pellets to fulfil the re-use of Dutch calcite as a replacement of the seeding material. For the test, initially the reactors were filled with Italian calcite and started up for 6 months. The calcite pellets were withdrawn from the reactor and grinded and sieved in an English factory therefor called English calcite. The sieved grains were introduced in the pellet softening reactor as a seeding material to acquire 100% pure CaCO_3 calcite pellets.

Pilot plant experiments were performed at the Weesperkarspel pilot plant. The experimental setup^[43] as shown in Figure 1 was used to conduct experiments on fluidisation behaviour. A 4 meter transparent PVC pipe with an inner diameter of 57 mm was used as fluidisation column. The bottom section of the pipe was fitted with a membrane with a mesh of 120 μm . This membrane functioned as the base of the bed, allowing water to flow through the bed as a plug flow reactor.

Three of the most important parameters were varied: water temperature, water flow and grain size. These three parameter were selected since they can easily and accurately be controlled. The fluidisation behaviour was examined measuring the flow at minimal fluidisation, expanded bed height, pressure drop and terminal falling velocity of the particular particles. The terminal settling behaviour was determined through adjusting the water temperature for various particles and for different grain sizes.

The water temperature was regulated by recirculating water through a buffer vessel connected to a boiler or cooler and thermostat. An overflow at the top of the reactor returns water to the buffer vessel. From the buffer vessel, water was pumped through both the boiler and the cooler, connecting to the thermostat which was set to the desired water temperature. For measuring water flow, two flow meters were used: a 0 to 100 L/h for lower flow regions and a 0 to 400 L/h for upper flow regions. A high pressure pump was used for the water circulation controlling the flow using a valve which is placed between the flow meters and the test column. All flow meters, temperature, pressure and scale have been calibrated. Bed heights were measured visually alongside the length of the reactor. Pressure difference was measured using taps on different heights. The taps were placed at 0, 10, 20, 30, 40, 50 and 100 cm above the membrane. The pressure drop was measured using a pressure difference meter connected the tap on the membrane and the tap on the desired height.

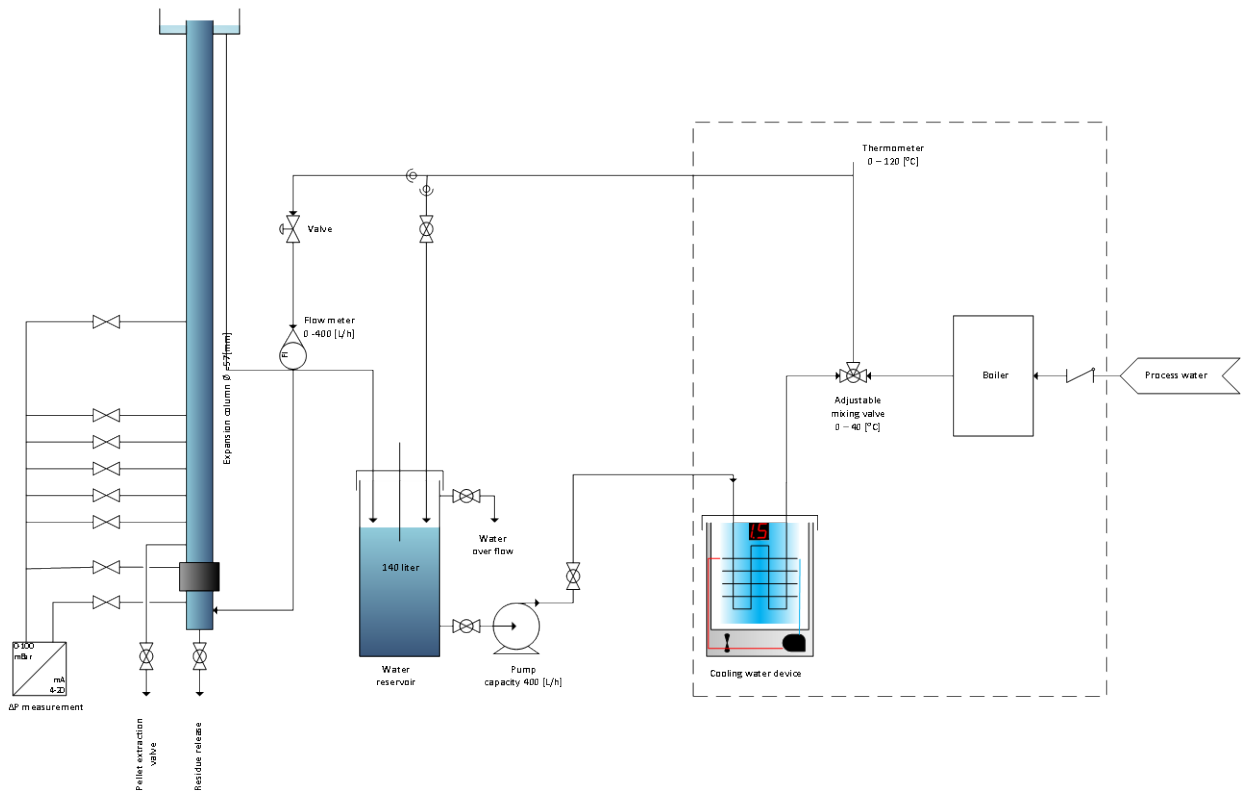


Figure 1 Experimental pilot set-up.

Fluid bed test materials

For this research predominantly calcite seeding material and calcite pellet grains were used for fluidisation and terminal settling experiments. In addition garnet pellets, seeding material i.e. garnet- and crystal sand, Italian calcite, broken and sieved pellets or English calcite and besides glass pearls were used. Calcite grains consists of pure chalk with a measured density of 2670 kg/m^3 .

To separate the particles to acquire more uniform samples, a device is used containing 20 sieve slides with increasing mesh openings. Sieving a bulk of calcite pellets into fractions allowed the grains size to be a parameter for the separate experiments. The following fractions were used (Table 1):

Table 1 Used grain fractions.

Mesh bottom sieve [μm]	Mesh top sieve [μm]	Average grain size [μm]
-	425	< 425
425	500	455
500	600	550
600	710	655
710	800	755
800	900	850
900	1120	1010
1120	1400	1260
1400	1700	1550
1700	2000	1850
2000	2360	2180
2360	-	2360 <

Experiments

To compare the theoretical models, two different experiments were conducted. More than 229 terminal velocity and 138 fluidisation experiments were carried out for the various grains. The pressure drop has been measured in 92 fluidisation experiments.

Average particle diameter

The applied sieve method is based on mass percentage of the particles divided over the slides. However, since the number of particles increase when the particle size decreases, also the number based average particle diameter can be estimated. This is due to the fact that in a fluidised bed smaller particles expand more compared to the larger particles. If N is the number of particles, and d_p their diameter with density ρ_p , then the following equation holds:

$$N = \frac{m}{\rho_p \frac{\pi}{6} d_p^3} (1 - \epsilon_0) \quad (43)$$

The particle volume from the sieve fraction j ($j=1$ to $j=k$) then is:

$$V_j = \frac{\pi}{6} d_j^3 \quad (\text{for one particle}) \quad (44)$$

The number based fraction x_j of sample j is:

$$V_j = \frac{N_j}{N_{tot}} = \frac{N_j}{\sum_{i=1}^k N_i} \quad (\text{number based fraction, straightforward Equation}) \quad (45)$$

From this the mass based fraction w_j can be calculated:

$$V_j = \frac{x_j V_j}{\sum_{i=1}^k x_i V_i} \quad (\text{mass based fraction}) \quad (46)$$

The number fraction from the mass fraction is:

$$x_j = \frac{\frac{w_j}{V_j}}{\sum_{i=1}^k \left(\frac{w_i}{V_i} \right)} \quad (47)$$

Now the average particle diameter can be calculated in two ways:

a) number based average:

$$\bar{d} = \sum_{i=1}^k x_i d_i \quad (48)$$

b) mass based average

$$\bar{d} = \sum_{i=1}^k w_i d_i \quad (49)$$

Generally, these averages are not equal. For the acquired sieve fractions (Table 4: nr. 1,2 and 8) the mass based average particle diameter is used and for mixtures (Table 4: nr. 3-7) with varying particle diameters fractions, the number based average particle diameter is calculated.

Particle density

Due to crystallisation of CaCO_3 at the particle surface the particle diameter increases. Since the density of the seeding material e.g. garnet sand is different from the density of calcium carbonate, the average density changes during the softening process. Using Equation 50 the average particle diameter is estimated.

$$\rho_p = \frac{d_g^3 \rho_g + (d_p^3 - d_g^3) \rho_c}{d_p^3} \quad (50)$$

Physical properties of water

The density and viscosity as a function of the water temperature is calculated through the default methods in the literature^{[26][40]}. The dynamic viscosity is given by the Vogel-Fulcher-Tammann Equation 51 (Table 2) according:

$$\mu = \frac{1}{c_5} e^{c_1 + \frac{c_2}{c_3 + (T + c_4)}} \quad (51)$$

Table 2 Vogel-Fulcher-Tammann coefficients.

c ₁	-3.7188
c ₂	578.919
c ₃	-137.546
c ₄	273.15
c ₅	1000

Particle density

The density of the pellets, seeding material and glass pearls is measured with a 50 mL pycnometer. Results can be found in Table 4.

Numerical Iteration

Four different models have been compared Ergun, Ergun-Adjusted, Carman-Kozeny and Richardson-Zaki for estimating the pressure drop, porosity and the particle size. The results can be found in Table 6.

The porosity in the Ergun Equation 24 is an implicit equation and is solved with the Excel with the GRG non-linear iteration method.

Although the Ergun-Adjusted can be solved explicitly, the n_{EA} coefficients in Equations 25, 29, and 30 are fitted to give the best results compared to the measured fluidisation data with the Excel solver.

To find the Carmán-Közény porosity an alternative method can be applied using Equation 52. Hereby the right-hand term, of Equation 38 is defined as $f(\varepsilon)$.

$$\varepsilon = c_1 - c_2 e^{-c_3 f(\varepsilon)^{c_4}} \quad 52$$

Table 3 Carmán-Közény porosity coefficients.

c ₁	=1,016-0,0436 n_{CK} + 0,0211 n_{CK}^2
c ₂	=0,753+0,101 n_{CK} + 0,190 n_{CK}^2
c ₃	=1,724-1,03 n_{CK} + 0,521 n_{CK}^2
c ₄	=0,841-0,710 n_{CK} + 0,211 n_{CK}^2

However, the porosity in Equation 38 is also estimated with the straightforward Excel goal seeker method. To find the optimal Carmán-Közény coefficients for the particle size estimation, initially in Equation 42 n_{CK} is changed until the slope diminished until zero since the particle diameter will not change during the experiments. Subsequently K_{CK} is adjusted to give the best match with the experimental fluidisation data.

For the pressure drop estimation in Equation 40 the solver is used to minimise the error = calculated – experimental data, in which the coefficients are numerically determined. Finally, the same principle with the solver method is used to estimate the best fitted Carmán-Közény coefficients or porosity prediction with Equation 41.

Terminal falling velocity experiments

The terminal falling velocity is the velocity a grain achieves by falling in an endless fluid. If the velocity of the fluid exceeds the terminal velocity of a particle, the particle will suspend or rise. All fractions in Table 1 were tested at for four different temperatures: 3, 14, 23 and 34°C.

Grains were dropped in the test column, measuring the time it takes for the grains to pass in a steady state velocity between two marks on the column (208 and 50 cm above the membrane). For every grain size each experiments was repeated several at least 6 times at different temperatures. The temperature was carefully controlled by flowing water through the column of the exact temperature before each experiment and regularly repeating this process throughout the experiment.

Fluidisation experiments

The fluidisation behaviour has been examined for a set of different grain sizes according Table 1 and Table 4. The test column was filled with 1 liter of uniform particles. The water temperature was kept constant during the experiments and was measured at the overflow of the column.

Starting the experiment, the cylinder was closed and the side of the column was gently tapped. The ‘fixed’ bed height was measured. The bed height and pressure difference were measured while increasing the water flow. The first 100 L/h were measured in steps of 10 L/h, continuing with steps of 20 L/h to a maximum of 400 L/h. Each grain size was tested at four temperatures. The acquired experimental data set consists of a matrix with varying temperature, grain size and flow and is required to compare the theoretical fluidisation models.

Full scale fluidisation experiments were possible at the full scale Weesperkarspel facility for Italian calcite (N=2) and English calcite i.e. broken and sieved calcite pellets (N=4). Washed seeding material has been weighted and dosed to an empty softening reactor in steps of 2 ton until 10 ton. The pressure drop at 50 cm and total pressure drop, water temperature, and water flow has been measured. The reactor has a diameter of 2.6 m and a height of 5.5 m. The water temperature was 17.7 °C. The water flow was increased from 30 to 100 m/h.

Bed porosity and expansion

Because the initial amount of grains is known, the fixed and fluid bed porosity and expansion can be calculated using:

$$\varepsilon_0 = 1 - \frac{m}{\frac{\pi}{4}D^2L_0\rho_p} \quad (53)$$

$$E = \frac{L}{L_0} = \frac{1-\varepsilon_0}{1-\varepsilon} \quad (54)$$

Wall effects

In the Richardson and Zaki^{[43][42]} Equation 2 wall effects can be taken into account. The most equations are empirical and take into account the wall effects of the vessel using a factor k. However, most equations have a low coefficient of correlation due to considerable data scatter of the experimental data.

The following models by Ladenburg-Faxen^[2], Fidleris and Whitmore^[9], Garside and Al-Dibouni^[9], Parodi-D-Felice, Francis^[43], Richardson-Zaki^[8] give the same results for k. The Ladenburg's^[9] improved Equation 55 is presented as:

$$\frac{v_t}{v_{t,(\varepsilon \rightarrow 1)}} = 1 - 2.104 \frac{d_p}{D} + 2.09 \left(\frac{d_p}{D}\right)^3 + 0.95 \left(\frac{d_p}{D}\right)^5 \quad \left(\frac{d_p}{D} < 0.2\right) \quad (55)$$

Modelling of full-scale fluid bed pellet reactors

Full scale reactor modelling through discretisation

In a full scale softening installation the crystallisation of CaCO_3 causes the particles to grow in size. In a steady-state situation, the particles are classified in size and particle density. The prediction of the fluid bed characteristics^[11] is complex due to the stratification of the particles caused by particle density, particle size and sphericity. To achieve a reliable state of the fluid bed, a discretisation model is proposed. In the discretisation model the bed is divided into smaller segments in which for each segment a specific particle diameter is specified. In the discretisation approach each segment corresponds with a bed height of 0.01 m. In every segment, the bed porosity, pressure drop, bed mass, flow regime, specific surface area and so on can be calculated in which profiles are acquired over the bed height. The total pressure drop and bed mass is the total sum of all the individual pressure drops and masses in the segments.

The chemical processes in the softening process mainly occurs at the bottom of the reactor. The upper part of the fluid bed aims to polish the remaining chemical reactions. Through discretisation over the bed height, detailed information can be acquired of the performance of the process. So using the discretisation model, at any time the bed condition can be checked and alarms can be generated in case the process variables are changed and leads to non-optimal fluid bed conditions.

Particle profile estimation

In case the overall pressure drop over the fluid bed is measured ΔP_{tot} and in addition the fluid bed height, a soft sensor can be used for estimating the particle size profile over the reactor bed height. In the discretisation model two points must be given. i.e. the set-point particle size at the bottom of the reactor and the smaller seeding material grain size at the top of the fluid bed, or a smaller fraction with a smaller grain size. These two points are (L_1, d_{p1}) and (L_2, d_{p2}) . Here $L_1 = 0$ (mostly) and d_{p1} = the pellet size at the bottom of the reactor. $L_2 =$ fluid bed height and d_{p2} = the particle size of the seeding material in the upper region of the bed. To estimate the pellets size at the bottom d_{p1} , one can use the pressure drop ΔP_{50} sensor.

The total pressure drop ΔP_c can be calculated with Equation 1 and the bed porosity with Equation 2.

Due to the relation between the porosity and the particle diameter (Equation 41), the particle diameter profile has been used in the model. Running the discretisation model with a linear profile according Equation 56 in:

$$d_p = p + qx \quad (56)$$

shows a too large overall pressure drop compared to the measured value ΔP_m .

Therefore a polynomial Equation 57 is proposed:

$$d_p = a + bx + cx^2 \quad (57)$$

By making the area under the polynomial curve smaller than the linear curve, a smaller pressure drop is acquired. Both the primitives of Equations 56 and 57 can easily be derived. The ratio of the linear and polynomial areas is:

$$v = \frac{a + \frac{b}{2}L + \frac{c}{3}L^2}{p + \frac{q}{2}L} \quad (58)$$

To estimate this ratio v the quotient of the measured and initially calculated pressure drop can be used:

$$v = \frac{\Delta P_m}{\Delta P_c} \quad (59)$$

The profile estimation coefficients now can be calculated with:

$$a = p \quad (60)$$

$$c = \frac{6(1-v)}{L^2v} p + \frac{3(1-v)}{Lv} q \quad (61)$$

$$b = \frac{6(v-1)}{Lv} p + \frac{(3-4v)}{v} q \quad (62)$$

By running the discretisation model for the second time an estimation of the particle profile is acquired. Using the bed height L and total pressure drop, this soft sensor makes it possible to gather information quickly for a probable particle profile in the reactor. This saves a lot of time since it is a much faster method compared with the individual sieve procedure. However, the latter is always more reliable. The minimum ratio can be calculated with:

$$V_{min} = \frac{4qL+6p}{3qL+6p} \quad (63)$$

Determining the flow regime

To determine if the solid-fluid system is homogeneous or heterogeneous, two different models have been imbedded.

According the Kunii-Levenspiel criterion^[3], the fluidisation is homogenous in case $Ku < 100$ and becomes heterogeneous if $Ku > 100$.

$$Ku = Ha Fr Re \frac{L}{D} \quad (64)$$

In which Ha (Harrison), Fr (Froude) and Re (Reynolds):

$$Ha = \frac{\rho_p - \rho_f}{\rho_f} \quad (65)$$

$$Fr = \frac{v_t^2}{gd_p} \quad (66)$$

$$Re = \frac{\rho_f d_p v_t}{\mu} \quad (67)$$

In addition, the fluid bed regime can be checked through the dynamic shock wave criterion^{[39][16]} for determining the transition from homogeneous to heterogeneous fluidisation^[38].

$$\sqrt{gd_p^3} \frac{(\rho_p - \rho_f)}{\mu} = \frac{4000}{\sqrt{\pi}} \frac{\epsilon_{mf}^{1.5}(1-\epsilon)^{1.5}}{\epsilon^{3.5}(1-\epsilon_{mf})^{0.5}(3-2\epsilon)} \quad Re < 2, \epsilon < 0.8 \quad (68)$$

$$\sqrt{gd_p^3} \frac{(\rho_p - \rho_f)}{\mu} = \frac{4000}{\sqrt{\pi}} \frac{\epsilon_{mf}^{2.1}(1-\epsilon)^{1.7}}{\epsilon^{4.1}(1-\epsilon_{mf})^{0.7}(3-2\epsilon)} \quad 2 < Re < 500, \epsilon < 0.8 \quad (69)$$

In which the left term N_{tr} is called the transition number. In case $N_{tr} < \text{right term of Equations 68 or 69}$, the flow regime is homogeneous and vice versa in case $N_{tr} \geq \text{right term}$, the flow regime is heterogeneous.

Performance of the fluid bed

For an optimal softening process the right amount of specific surface area in the lower 0.50 m section of the reactor is necessary. The specific surface area is the total existing area per volume fluid bed unit. For instance, too large particles can adversely affect the crystallisation process due to a decreasing specific surface area^[43]. In case the porosity profile is known, the specific surface area can be determined in the critical parts of the fluidised bed reactor with:

$$A_s = \frac{6(1-\epsilon)}{d_p} \quad (70)$$

And in addition, the space velocity^[25] A_c i.e. the number of reactor volumes of feed at specified conditions which can be treated in unit acquired with Equation 71:

$$A_c = \frac{v_l}{\epsilon} A_s \quad (71)$$

Depending on the particle size and temperature, a critical value of A_s is approximately $2200 \text{ m}^2/\text{m}^3$ and of A_c approximately 100 s^{-1} . It is very important that the fluid flow is higher than the minimal fluidisation velocity. So using the discretisation model, at any time the bed condition can be checked and alarms can be generated in case the process variables are changed and leads to non-optimal fluid bed conditions.

The crystallisation process mainly occurs in the lower section of the reactor, the specific surface area can be used as a good indicator to monitor the performance of the conversion process. The polishing effect of the fluid bed in the remaining part of the reactor can be monitored with the space velocity.

RESULTS AND DISCUSSION

Particle size

From the sieve experiments the following average particle diameter is acquired:

For garnet sand: 0.25 mm (mass based) and 0.23 mm (number based), for Italian calcite: 0.48 mm (mass based) and 0.45 mm (number based) for more results see Table 1 and Table 4. In particular for mixtures with varying grain sizes, the number based method gives better results i.e. garnet sand and will be chosen.

Table 4 Physical particle properties.

Nr.	Grain	Density [kg/m ³]	Grain diameter mass based average [mm]	Grain diameter number based average [mm]	Fixed bed porosity [m ³ /m ³]
1	Calcite pellets	2670	**)	-	0.40
2	Garnet pellets*)	2700	**)	-	0.40
3	Italian calcite	2670	0.48	0.45	0.42
4	English calcite (broken calcite pellets)	2600	0.47	0.36	0.44
5	Garnet sand mesh80	4114	0.25	0.23	0.43
6	Garnet sand mesh30/60	4192	0.33	0.29	0.42
7	Crystal sand	2626	0.51	0.49	0.40
8	Glass pearls	2500	**)	-	0.40

*) The average particle density depends on the diameter of the inner seeding material, the density of CaCO₃ and the pellet diameter according Equation 50.

***) Sieve fractions mentioned in Table 1 are used therefore, no overall average grain diameter applies.

Calibration of theoretical models with experimental data

The data derived from both the expansion and terminal settling experiments is used to calculate the pressure difference, porosity of the expanded bed and average particle size. The pressure difference is compared with the measured value. This porosity is compared with the porosity derived directly from the data and the average particle diameter with the sieve fractions. Additionally, data sets from earlier experiments were used to calibrate the different models.

To compare the models with the practice, the deviations between the models is calculated, compared with the experimental data and plotted against the Reynolds number or Archimedes number. From these results it can be concluded that the model of Richardson-Zaki with 1% error is the most accurate model to predict the porosity. The statistical results for the estimation of the pressure drop and average particle size are given in Table 5 and model coefficients in Table 6, Table 7 and Table 8.

Table 5 Fluidisation prediction models deviations.

Soft sensor	Statistics	Ergun	Ergun-Adjusted*)	Carmán-Közény*)	Richardson-Zaki
Pressure difference N=83	Error	20%	14%	7%	13%
Fluid bed porosity N=135	Error	5%	2%	5%	1%
Particle diameter N=101	Error	42%	10%	4%	4%

*) Calibrated models. The results of the models with the default coefficients were less accurate and had worse deviations.

The models of Ergun will not be selected for the full-scale model due to their larger errors. In several cases the Carmán-Közény coefficients could not be found because the fitting did not converge and unrealistic results were acquired. These values have been omitted. The Richardson-Zaki equations do not require

adjustable coefficients at all. Therefore, the Richardson-Zaki equations 40, 41 and 42 are preferred for the fluid model-based prediction of the fluid bed state.

Table 6 Fluidisation model coefficients.

Soft sensor	Ergun	Ergun-Adjusted*)	Carman-Kozeny*)	Richardson-Zaki
Pressure difference	Eq. 20	Eq. 29	Eq. 37	Eq. 40 (**)
	Explicit	Explicit	Explicit	Explicit
	-	$n_{EA}=5.15$	$n_{CK}=0.877, K_{CK}=3.96$	See Table 8
Fluid bed porosity	Eq. 24	Eq. 30	Eq. 38 and 52	Eq. 41
	Implicit	Explicit	Implicit and Explicit	Explicit
	-	$n_{EA}=5.24$	$n_{CK}=0.815, K_{CK}=3.07$	See Table 8
Particle diameter	Eq. 25	Eq. 25	Eq. 39	Eq. 42
	Explicit	Explicit	Explicit	Explicit
	-	$n_{EA}=4.54$	$n_{CK}=0.884, K_{CK}=3.88$	See Table 8

*) Calibrated models.

**) Only for fluid bed conditions, not for fixed bed state.

Determining the Richardson-Zaki coefficients

The Richardson-Zaki porosity prediction requires the terminal settling velocity and the index n_{RZ} . The terminal velocity is obtained through plotting Reynolds terminal $\ln(Re_t)$ or the dimensionless terminal velocity $\ln(\dot{u})$ against Archimedes $\ln(Ar)$ from which a linear relation is acquired Figure 2 with slope and intercept.

Table 7 Richardson-Zaki terminal settling coefficients.

Grains	$Re_t = e^{c_1} Ar^{c_2}$	$\dot{u} = \alpha Ar^\beta$	$C_D = \alpha Re_t^\beta$
Equations	Eq. 18, (5 and 7)	Eq. 15, (16 and 7)	Eq. 14, (10 and 5)
For all data	$c_1=-1.213, c_2=0.655$	$\alpha=0.0329, \beta=0.925$	$\alpha=8.75, \beta=-0.478$
Correlation coefficient	$r^2=0.996$	$r^2=0.983$	$r^2=0.962$
Pellets, calcite and garnet sand	$c_1=-1.215, c_2=0.654$	$\alpha=0.0325, \beta=0.926$	$\alpha=8.80, \beta=-0.478$
Correlation coefficient	$r^2=0.997$	$r^2=0.986$	$r^2=0.969$

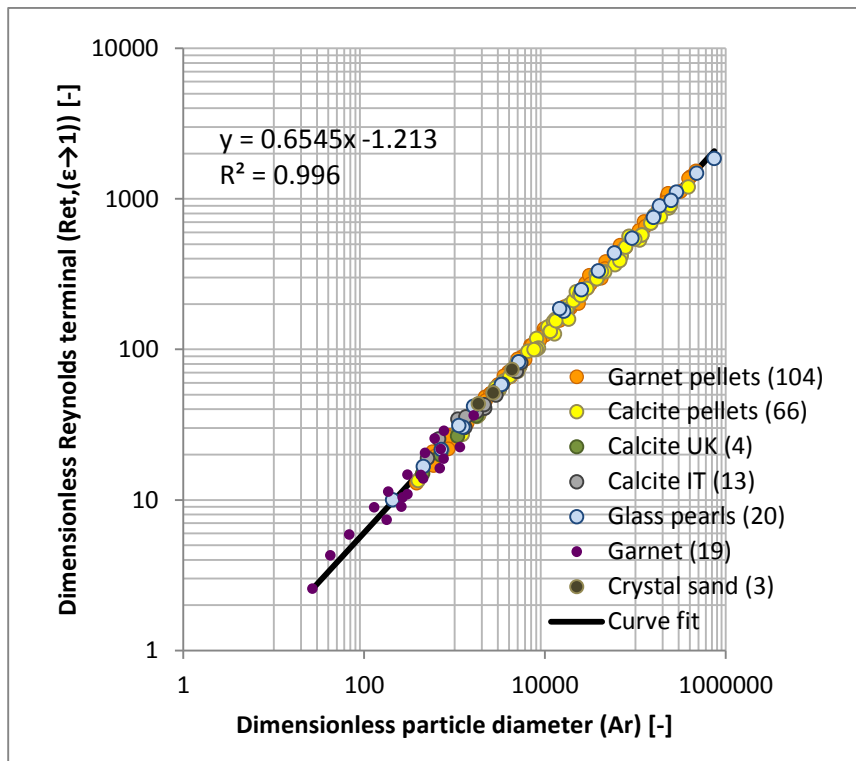


Figure 2 Linear plot of 229 terminal settling velocity experiments.

From the Richardson-Zaki terminal settling coefficients (Table 7) Equation 16 (Reynolds vs Archimedes) is chosen due to the highest correlation coefficient.

The Richardson-Zaki hindering index n_{RZ} was calculated with Equation 2 in which the wall effects have been taken into account using Equation 55. Combining the most reliable estimation method of terminal settling velocity v_t was Equation 17. To acquire the model coefficient of N_{RZ} Equation 9 has been applied, which can be linearized by taking logarithms.

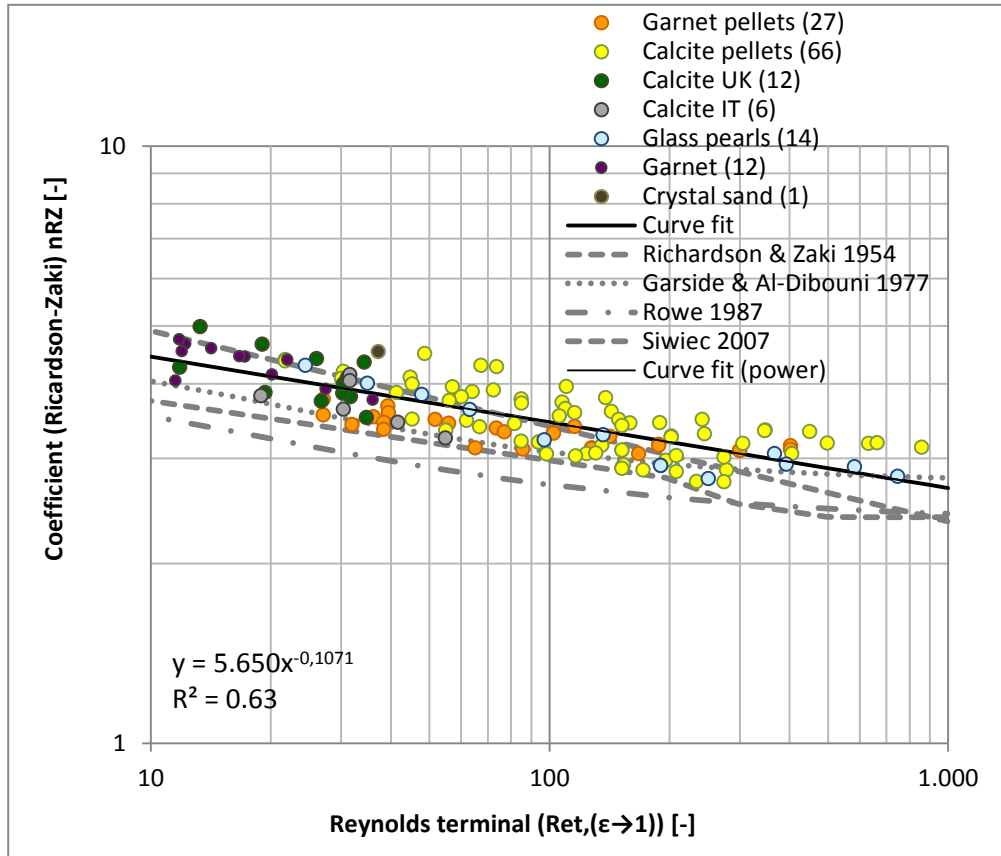


Figure 3 Richardson-Zaki coefficient n_{RZ} plot of 138 fluidisation experiments.

Table 8 Richardson-Zaki n_{RZ} model coefficients: $n_{RZ} = a_1 Re_t^{a_2}$, Equation 9.

Grains	Coefficients	Correlation coefficient
For all data	$a_1=5.72, a_2=-0.110$	$r^2=0.66$
Pellets*), calcite**) and garnet sand	$a_1=5.65, a_2=-0.107$	$r^2=0.63$
Pellets*) and garnet sand	$a_1=5.38, a_2=-0.097$	$r^2=0.53$
Pellets*)	$a_1=5.12, a_2=-0.087$	$r^2=0.42$
Garnet sand	$a_1=6.91, a_2=-0.164$	$r^2=0.66$
Italian calcite	$a_1=6.72, a_2=-0.170$	$r^2=0.41$
English calcite	$a_1=6.92, a_2=-0.163$	$r^2=0.35$
Glass pearls	$a_1=5.83, a_2=-0.116$	$r^2=0.85$

*) Both garnet pellets as calcite pellets.

**) Both Italian calcite as English calcite.

The correlation coefficients in Table 8 are rather low. Nevertheless the literature^{[35][9][29]} often mentions low r^2 values in the range of 0.40 to 0.95 for natural grains probably due to the non-spherical shape and varying surface roughness.

The Richardson-Zaki model has been chosen as the most reliable and explicit model. The coefficients $c_1=-1.215$ and $c_2=0.654$ were determined from the terminal settling experiments for pellets, garnet sand and

calcite using Equation 18 or 19. The coefficients n_{RZ} have been acquired from the fluidisation experiments also for pellets, garnet sand and calcite: $a_1=5.65$ and $a_2=-0.107$ using equation 9. In this way the model-based prediction of the fluid bed state with the Richardson-Zaki model is possible in Excel.

Fluidisation regime

Two fluidisation regime models have been used to determine the state of the fluid bed during fluidisation experiments. According the Kunii-Levenspiel criterion with Equation 64 homogeneous fluidisation occurred for 95.8% and according to the dynamic shock waves criterion using Equations 68 or 69 homogeneous fluidisation occurred for 99.4%. At higher superficial velocity e.g. above 120 m/h, heterogeneous fluidisations occurs.

Sphericity

The sphericity ϕ_s according the Wen-Yu^[43] Equations 21 and 22 and besides the Limas-Ballesteros^[4] Equation 23 has been calculated for seeding material.

Table 9: Sphericity of seeding material.

Grain	Wen-Yu Eq. 21	Wen-Yu Eq. 22	Limas-Ballesteros Eq. 23
Italian calcite	0.87 ± 0.09	0.79 ± 0.05	0.91 ± 0.09
English calcite	0.72 ± 0.07	0.70 ± 0.04	0.77 ± 0.06
Garnet sand mesh 80	0.83 ± 0.14	0.77 ± 0.07	0.88 ± 0.11
Garnet sand mesh 30/60	1.04 ± 0.12	0.88 ± 0.07	1.07 ± 0.13
Crystal sand	0.79 ± 0.07	0.74 ± 0.01	0.84 ± 0.02

In the literature^[41] the sphericity or a shape factor is proposed to solve the problem of not completely round particles. Applying the Equations 21 and 22 according to Ergun^[15] did not result in better results. The main reason is that the not ideal fluidisation behaviour of the particles isn't caused by only the sphericity, also surface imperfection and the position of the particles contribute. Therefore the use of shape factors for particle diameter is not advised. It's not clear if the calculated sphericity factors in Table 9 can be used as a shape factor to correct for not ideal roundness of the seeding grains due to the significant error. Therefore, in this research the sphericity factor $\phi_s=1$ is used.

Validation

For the validation discretisation modelling of the full-scale Weesperkarspel plant was done using the average particle size estimation method with the linear Equation 56 versus parabolic Equation 57. The discretisation model divides the bed height in segments of 0.01 m bed height in which the state is calculated assuming that the bed condition in every segment is uniform. During the filling process of the softening reactor with English calcite the temperature, water flow, total fluid bed height, pressure drop and pressure difference at 0.50 m as well as the dosed mass were measured. The model requires the bottom grain size and size at the upper region of the bed. The initial point for the model becomes: ($L_1=0$ m, $d_{p1}=0.55$ mm) and ($L_2=3.88$ m, $d_{p2}=0.30$ mm). At first the linear profile is used as input values for the discretisation model to determine the theoretically total pressure drop. The pressure drop $\Delta P_{tot,th}=11.6$ kPa and $m=10.9$ ton. This is compared with the actual measured value $\Delta P_{tot,m}=11.0$ kPa and $m_{th}=10.0$ ton resulting in a ratio $v=0.95$. The second parabolic profile is used for the input of the discretisation model resulting in $\Delta P_{tot,th}=10.8$ kPa and $m_m=10.2$ ton. Subsequently the different process parameters are plotted in Figure 4. The specific surface area has a maximum at a certain 1.30 m. Below this height the specific surface area decreases because then the pellet diameter is decisive and above this height A_s increases due to the more decisive porosity.

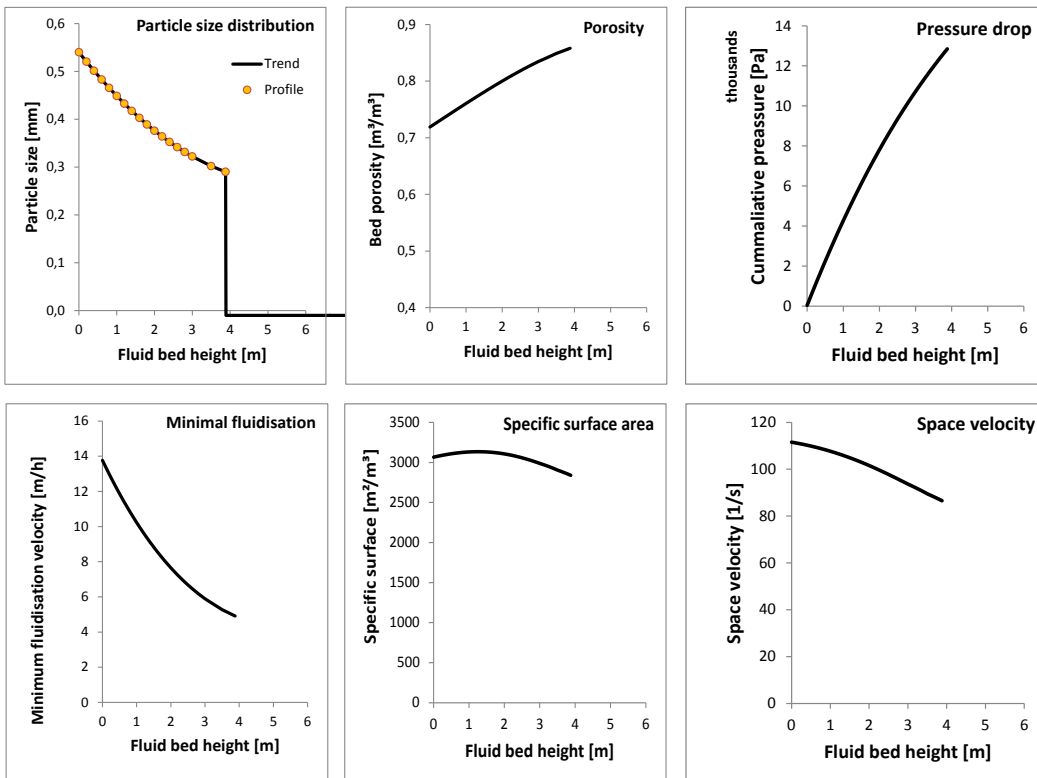


Figure 4: Particle size distribution over the bed height [mm] in the Weesperkarspel softening reactor 2 and other profiles for the English calcite full-scale fluidisation test in September 2014. $m_p=10$ ton, $Q_w=500$ m³/h, $L=3.9$ m, $D=2.6$ m, $T=16$ °C, $\Delta P_{50}=2.1$ kPa, initial sand washing mass loss 2%, sieve analyses $d_{10}=0.30$ mm. See Table 4.

Another validation had been done for the classic softening process with garnet pellets with a particle size of 1.0 mm. The initial point for the model becomes: ($L_1=0$ m, $d_{p1}=1.0$ mm) and ($L_2=3.40$ m, $d_{p2}=0.20$ mm). The smallest particles in the fluid bed reactor are 0.20 mm due to the washing procedure of the garnet sand. At first the linear profile is used as input values for the discretisation model to determine the theoretically total pressure drop. The pressure drop $\Delta P_{tot,th}=18.4$ kPa. This is compared with the actual measured value $\Delta P_{tot,m}=16.3$ kPa resulting in a ratio $v=0.86$. And the second parabolic profile is used for the input of the discretisation model resulting in Figure 5. For optimal softening conditions a large specific surface area is wanted in the lowest region of the reactor. In Figure 4 this is the case, however in the contrary showed in Figure 5 where the specific surface area is larger in the top of the fluid bed. This is due to the larger pellets at the bottom and the considerable smaller garnet particles at the top.

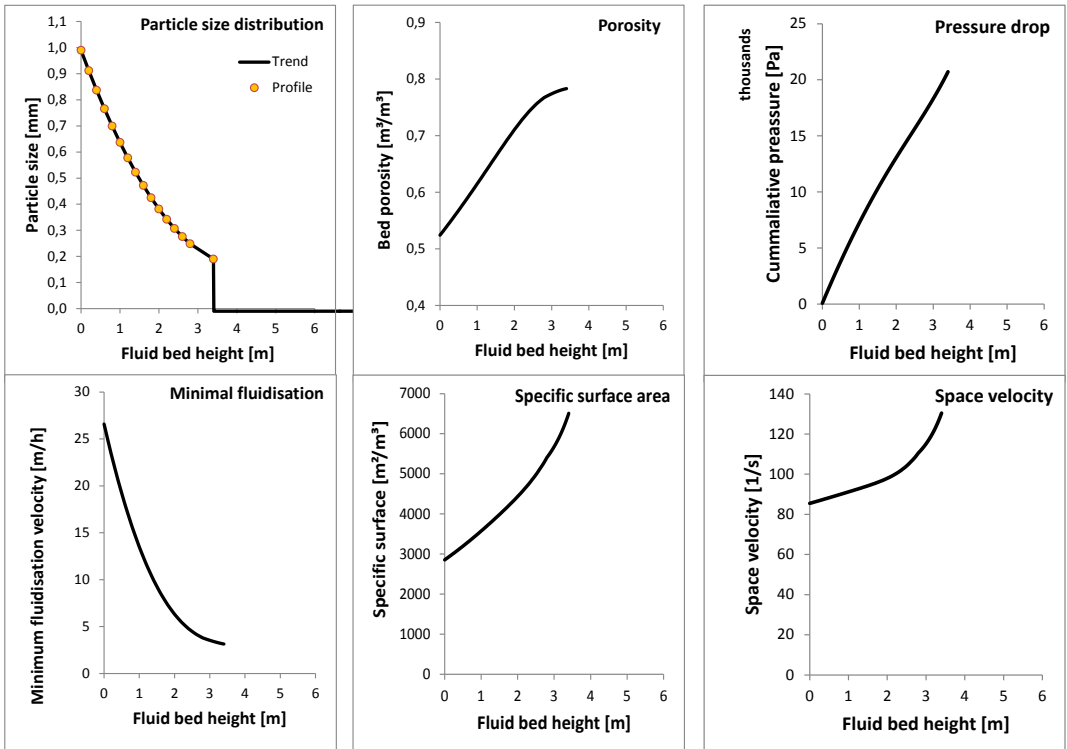


Figure 5: Particle size distribution over the bed height [mm] in the Weesperkarspel softening reactor 1 and other profiles for the garnet pellets full-scale fluidisation test in March 2005. $Q_w=300 \text{ m}^3/\text{h}$, $L=3.4 \text{ m}$, $D=2.6 \text{ m}$, $T=5 \text{ }^\circ\text{C}$, $\Delta P_{\text{tot}}=16.3 \text{ kPa}$, initial garnet sand washing mass loss 1%, sieve analyses $d_{10}=0.20 \text{ mm}$. see Table 4.

Validation pressure difference full scale reactor

Initially, the bed porosity is derived from pressure difference measurement ΔP_{50} in the lowest 0.50 meter of the reactor and calculated with Equation 28. With Equation 40 for Richardson-Zaki the pressure difference is calculated and plotted in Figure 6. The observed error is mainly caused by the sensitivity of the pressure measurement.

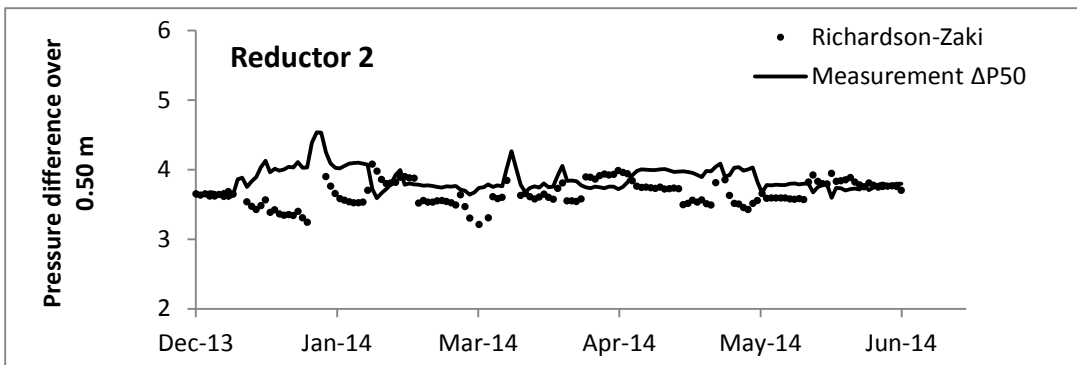


Figure 6 Pressure difference ΔP_{50} estimation for Weesperkarspel reductor 2.

Validation porosity full scale reactor

Using Equation 41 for Richardson-Zaki the bed porosity in the lowest region of the reactor is calculated and plotted in Figure 7. The porosity derived from pressure difference measurement ΔP_{50} is slightly higher than the estimated porosity by Richardson-Zaki and can be explained since the actual pressure is a pressure difference measurement between 0.65 m and 0.15 m from the bottom. One explanation could be that in the reactor the particle profile over the reactor bed means that the largest particles are at the bottom of the reactor and the smallest in the upper region of the bed. Therefore, the particles are somewhat smaller and the

porosity slightly higher. The second explanation could be an off-set of the pressure difference measurement device.

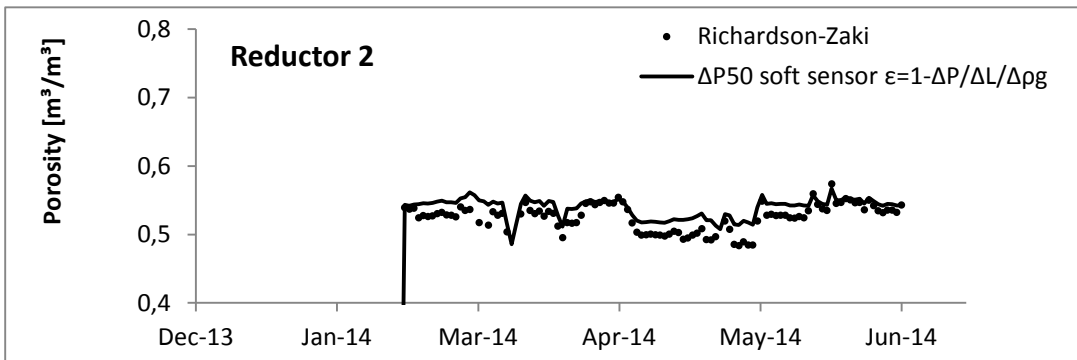


Figure 7 Porosity estimation for Weesperkarspel reductor 2.

Validation average particle size full scale reactor

Initially, the bed porosity is derived from pressure difference measurement in the lowest 0.50 meter of the reactor and using Equation 28. Using Equations 42 for Richardson-Zaki the average particle size is calculated and plotted in Figure 8.

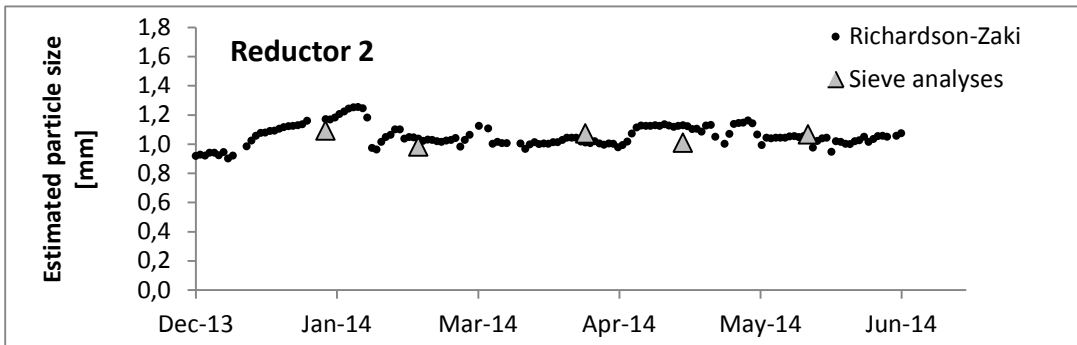


Figure 8 Particles size estimation for Weesperkarspel reductor 2.

The particle size was estimated for the Weesperkarspel pellet softening reactor 2 during six months. Pellets were withdrawn from the reactor for analysing purposes. The particle size soft sensor is very sensitive for the performance of the pressure difference measurement device due to the small interval of ΔP . Nevertheless the soft sensors can be used online to follow the bed condition of the fluid bed. The soft sensor should not be used to acquire detailed information about the particles size distribution, than sieve analyses are required.

CONCLUSIONS

Fluidised bed reactors are used for water softening in drinking water treatment plants. To improve market value of pellets and the sustainability of the process, garnet sand has been replaced by calcite as seeding material. No data is available to predict the fluidisation behaviour under different conditions for calcite pellets or calcite as a seeding material. Pilot and full scale fluidisation experiments besides terminal velocity experiments have been carried out.

The results of the fluidisation and terminal settling experiments were compared to several modelling approaches of Ergun, Ergun-Adjusted, Carmán-Közény and Richardson-Zaki. Richardson-Zaki model is the most reliable fluid bed model under conditions measured.

It can be concluded that applying a discretisation model in Excel, the current operation of the treatment softening can be improved by predicting the optimal fluidisation behaviour using the preferred Richardson-Zaki model.

To predict mixtures of particle with varied particle size, the numbered based average particle diameter is much more reliable compared with the default mass based average diameter.

The use of the developed soft sensors, in which the porosity, pressure drop and average particle size can be estimated, contribute to a highly automated softening process for control of flows.

Waternet can apply the improved fluid bed model as a soft sensor to achieve optimal fluid bed conditions and which will result in less caustic soda dosing. The Richardson-Zaki equations do not require adjustable coefficients. Therefore, the Equations 40, 41 and 42 are preferred for the model-based prediction of the fluid bed state. The coefficients $c_1=-1.215$ and $c_2=0.654$ and the coefficients $a_1=5.65$ and $a_2=-0.107$ should be used in the Richardson-Zaki model.

RECOMMENDATIONS

The Richardson-Zaki coefficient is dependent on the Reynolds terminal number. It should be examined if the Archimedes number could be a solution to avoid implicit equations.

For further research, it is advisable to pay attention to the sphericity ϕ_s of the particles. In this article the sphericity has not been accounted for. Also the residence time distribution can be a point of interest.

To improve the reliability of the soft sensors, more attention is needed in the validation, development, optimisation and implementation in the full scale softening process.

Symbols

α, β	Coefficients in the Richardson-Zaki index	[-]
a, b, c	Coefficients in quadratic particle profile estimation model	[-]
Ar	Dimensionless particle diameter, Archimedes number	[-]
A_c	Space velocity, number of reactor volumes	$[\text{m}^2/\text{m}^3 \cdot \text{m/s}] = [1/\text{s}]$
A_s	Specific surface area	$[\text{m}^2/\text{m}^3]$
C_D	Drag coefficient	[-]
D	Column or vessel diameter	[m]
d_p	Average particle diameter	[m]
d_g	Average seeding material diameter	[m]
ε	Porosity or voidage of the system	$[\text{m}^3/\text{m}^3]$
ε_o	Fixed bed porosity	[-]
ε_{mf}	Porosity at minimum fluidisation	[-]
E	Bed expansion	[%]
f	Carmán-Közény correlation for Reynolds porosity corrected	[-]
g	Gravitation force	$[\text{m/s}^2]$
k	Wall effects correction factor	[-]
K_{CK}	Carmán-Közény coefficient	[-]
Ku	Kunii-Levenspiel criterion parameter	[-]
L	Fluid bed height	[m]
L_0	Fixed bed height	[m]
m	Mass	[kg]
n_{EA}	Ergun-Adjusted coefficient	[-]
n_{RZ}	Richardson-Zaki coefficient	[-]
n_{CK}	Carmán-Közény coefficient	[-]
N	Total number of particles / Total number of experiments	[#]
N_{tr}	Transition number in the dynamic shock wave criterion	[-]
ρ_f	Fluid density	$[\text{kg}/\text{m}^3]$
ρ_p	Particle density	$[\text{kg}/\text{m}^3]$
ρ_g	Seeding material density	$[\text{kg}/\text{m}^3]$
ρ_c	Density of calcium carbonate	$[\text{kg}/\text{m}^3]$
p,q	Coefficients in linear particle profile estimation model	[-]
ΔP	Pressure drop head loss	[kPa]
ΔP_c	Calculated pressure drop using discretisation	[kPa]
ΔP_m	Measured pressure drop over the total fluid bed	[kPa]

ΔP_x	Pressure drop head loss over column length x	[kPa]
ΔP_{tot}	Total pressure drop over the bed	[kPa]
Q_w	Water flow	[m ³ /h]
Re_h	Reynolds number (friction)	[-]
Re_0	Reynolds number (particle)	[-]
Re_p	Reynolds number (particle porosity)	[-]
Re_t	Reynolds for terminal velocity conditions	[-]
Re_ε	Reynolds corrected for the porosity	[-]
r_m	Logarithmical average diameter	[m]
σ	Standard deviation	[m]
σ^2	Associated variance	[m ²]
ϕ_s	Sphericity, shape of diameter correction factor	[-]
t	Time	[s]
T	Temperature	[°C]
T	Tortuosity	[-]
\hat{u}	Dimensionless particle terminal settling velocity	[-]
v	Ratio in particle profile estimation model	[-]
v_l	Linear superficial velocity or empty tube fluidisation velocity	[m/s]
v_t	Terminal particle settling velocity	[m/s]
$v_{t,(\varepsilon \rightarrow 1)}$	Free falling settling velocity of a particle in an infinite solution	[m/s]
μ	Dynamic fluid viscosity	[kg/m/s]
μ_w	Weighted average of the particle diameter	[m]
V	Volume	[m ³]
x	Average particle diameter between top and bottom sieves	[m]

References

- [1] Akgiray, O. & Soyer, E., 2006, "An evaluation of expansion equations for fluidized solid-liquid systems", *IWA Publishing, Journal of Water Supply: Research and Technology – AQUA*, **55**(7–8), pp. 517-526.
- [2] Bird, R.B., Stewart, W.E. & Lightfoot, E.N., 2001, "Transport phenomena", John Wiley & Sons, Inc. International 2nd Edition, ISBN: 15BN 0-471-41077-2.
- [3] Carmán, P.C., 1937, "Fluid flow through granular beds." *Transactions, Institution of Chemical Engineers*, London, 15, pp. 150-166.
- [4] Chianese, A., Frances, C., Di Bernardino, F. & Bnmo, L., 1992, "On the behaviour of a liquid fluidized bed of monosized sodium perborate crystals", *Chemical Engineering Journal*, **50**, pp. 87-94.
- [5] Clift, R., Grace, J.R. & Weber, M.E., 1978, "Bubbles, drops, and particles", Academic Press, San Diego, CA..
- [6] Concha, F. & Almendra, E.R., 1979a, "Settling velocity of particulate systems, 1., Settling velocity of individual spherical particles," *International Journal of Mineral Processing*, **5**, pp. 349-369.
- [7] Concha, F. & Almendra, E.R., 1979b, "Settling velocity of particulate systems, 2., Settling velocity of suspension of spherical particles," *International Journal of Mineral Processing*, **6**, pp. 31-41.
- [8] Coulson, J.M. & Richardson, J.F., 1989, "Chemical Engineering", Pergamon Press, Volume 2, 3rd edition, ISBN: 0-08-02291-0.
- [9] Dharmarajah, A.H., 1982, "Effect of particle shape on prediction of velocity voidage relationship in fluidized solid-liquid systems", Iowa State University, Retrospective Theses and Dissertations. Paper 7535.
- [10] Dietrich, W.E., 1982, "Settling velocity of natural particles", *Water Resources Research*, **18**(6), pp. 1615-1626.
- [11] Di Felice, R., 1995, "Hydrodynamics of Liquid Fluidisation", *Chem. Eng. Sci.*, **50**(8), pp. 1213-1245.

- [12] Di Felice, R. & Kehlenbeck, R., 2000, "Research News, Sedimentation velocity of solids in finite size vessels", *Chem. Eng. Technol*, **23**(12), pp. 1123-1126.
- [13] Dijk, van, J.C. & Wilms, D.A., 1991, "Water treatment without waste material-fundamentals and state of the art of pellet softening", *Journal Water Supply, Research and Technology: AQUA*, **40**(5), pp. 263-280.
- [14] Dirken, P., Baars, E.T., Graveland, A.J. & Woensdregt, C.F., 1990, "On the crystallization of calcite {CaCO₃} during the softening process of drinking water in a pellet reactor with fluidized beds of quartz, garnet and calcite seeds", *11th Symposium on Industrial Crystallization*.
- [15] Ergun, S., 1953, "Fluid flow through packed columns", *Chem. Eng. Prog.*, **48**(2), pp. 89-94.
- [16] Gibilaro, L.G., 2001, "Fluidization dynamics", ISBN: 0 7506 5003 6.
- [17] Gibilaro, L.G., Di Felice, R., Walgram, S.P. & Foscolo, P.U., 1985, "Generalized friction factor and drag coefficient correlations for fluid-particle interactions", *Chem. Eng. Sci.*, **40**(10), pp. 1817-1823.
- [18] Graveland, A.J., Dijk, van, J.C., Moel, de, P.J. & Oomen, J.H.C.M., 1983, "Developments in water softening by means of pellet reactors", *Journal AWWA*, **75**(12), pp. 619-625.
- [19] Grbavčić, Ž.B., Garic, R.V., Hadzismajlovic, E., Janovics, S., Vuković, D.V., Littman, H. & Morgan, M.H., 1991, "Variational model for prediction of the fluid-particle interphase drag coefficient and particulate expansion of fluidised and sedimenting beds", *Powder Technology*, **68**, pp. 199-211.
- [20] Hofman, J., Kramer, O. J. I., van der Hoek, J. P., Nederlof, M. & Groenendijk, M. 2007 Twenty years of experience with central softening in The Netherlands: *Water quality - Environmental benefits – Costs.*, Water21, July, pp. 21 –24.
- [21] Khan, A.R. & Richardson, J.F., 1989, "Fluid-particle interactions and flow characteristics of fluidized beds and settling suspensions of spherical particles", *Chem. Eng. Comm.* **78** pp. 111.
- [22] Kim, B.H., 2003, Modelling of hindered settling column separations", Ph.D. thesis, pp. 1-186.
- [23] Kramer, O.J.I., 2014, "Circular economy in drinking water treatment: re-use of grinded pellets as seeding material in the pellet softening process", Conference poster presentation at *the IWA World Water Congress and Exhibition*, Lisbon.
- [24] Montgomery, J., 1985, "Water treatment, Principles & Design", John Wiley & Sons, New York, USA.
- [25] Levenspiel, O., 1999, "Chemical reaction engineering", John Wiley & Sons, 3rd ed., ISBN: 0-471-25424-X.
- [26] Perry, R.H., Green, D., 1984, "Perry's chemical engineers handbook", McGraw-Hill Int. edition, 50th ed., ISBN 0-07-Y66482-X.
- [27] Richardson, J.F. & Zaki, W.N., 1954, "Sedimentation and fluidisation part I", *Trans. Inst. Chem. Eng.*, **32**, pp. 35-53.
- [28] Richardson, J.F. & Zaki, W.N., 1954, "The sedimentation of a suspension of uniform spheres under conditions of viscous flow", *Chem. Eng. Sci.*, **3**, pp. 65-73.
- [29] Rowe, P.N., 1987, "A convenient empirical equation for estimation of the Richardson-Zaki exponent", *Chem. Eng. Sci.*, **42**, nr. 11, pp. 2795-2796.
- [30] Schagen, K.M., Rietveld, L.C. Babuška, R. Kramer, O.J.I., "Model-based operational constraints for fluidised bed crystallisation", *Water Research*, 2008, **42**, pp. 327–337.
- [31] Schagen, K.M., 2009, "Model-Based Control of Drinking-Water Treatment Plants", ISBN: 978-90-8957-008-6, Ph.D. thesis.
- [32] Schetters, M.J.A., 2013, "Grinded Dutch calcite as seeding material in the pellet softening process", Master thesis, Faculty of Civil Engineering and Geosciences, Delft University of Technology, Delft, the Netherlands.
- [33] Schetters, M.J.A., Hoek, van der, J.P., Kramer, O.J.I., Kors, L.J., Palmen, L.J., Hofs, B. & Koppers, H., 2014, Circular economy in drinking water treatment: re-use of grinded pellets as seeding material in the pellet softening process", In Press..
- [34] Schiller, L., & Naumann, A., 1933. "Über die grundlegenden Berechnungen bei der Schwerkraftaufbereitung", *Ver. Deut. Ing.* **77**, pp. 318–320.
- [35] Siwiec, T., 2007, "The experimental verification of Richardson-Zaki law on example of selected beds used in water treatment", *Electronic Journal of Polish Agricultural Universities*, **10**(2), pp 49-54.

- [36] Turton, R. & Levenspiel, O., 1986, "A short note on the drag correlation for spheres", *Powder Technology*, **47**, pp. 83-86.
- [37] Veen, van der, C. & Graveland, A.J., 1988, "Central softening by crystallization in a fluidized bed process", *Journal AWWA*, 1988, June, pp. 51-58.
- [38] Verloop, J. & Heertkes, P.M., 1973, "The onset of fluidization", *Powder Technology*, **7**, pp. 161-168.
- [39] Verloop, J. & Heertjes, P.M., 1969, "Shock waves as criterion for the transition from homogeneous to heterogeneous fluidization", Laboratory Chemical Engineering, Delft University of Technology.
- [40] Weast, R.C., 1984, "Handbook of Chemistry and Physics", CRC Press, 60th edition ISBN: 0-8493-0460-8.
- [41] Wen, C.Y. & Yu, Y.H., 1966, "Mechanics of fluidization, *Chem. Eng. Prog. Symp. Series*, **62**, pp. 100-111.
- [42] Yang, J. & Renken, A., 2003, "A generalized correlation for equilibrium of forces in liquid-solid fluidized beds", *Chem. Eng. J.*, **92**, pp. 7-14.
- [43] Yang, W., 2003, "Handbook of Fluidization and Fluid-Particle Systems", pp 49-54, pp. 138-142.

Acknowledgements

Special thanks to Rob de Wit, Ismail Boutaleb, Marc Schetters, Mark Joosten, Jan Hangelbroek, Ruud Kolpa, Jos Hooft, Pieter Nijdam, Fred van Schooten, Jan van Duijvenbode, Hans van Pinksteren, Gerrit Jan Zweere, Sven Kramer and Ben Vermeulen for their contribution to this research.